Please do not adjust margins

ARTICLE

Self-assembled multivalent (SAMul) ligand systems with enhanced stability in the presence of human serum

Received 00th January 20xx,
Accepted 00th January 20xx

DOI: 10.1039/x0xx00000x

Marta Tena-Solsona,[a] Domenico Marson,[b] Ana Campo Rodrigo,[a] Erik Laurini,[b] Sabrina Pricl,*[b] and David K. Smith*[a]

Self-assembled cationic micelles are an attractive platform for binding biologically-relevant polyanions such as heparin. This has potential applications in coagulation control, where a synthetic heparin rescue agent could be a useful replacement for protamine, which is in current clinical use. However, micelles can have low stability in human serum and unacceptable toxicity profiles. This paper reports the optimisation of self-assembled multivalent (SAMul) arrays of amphiphilic ligands to bind heparin in competitive conditions. Specifically, modification of the hydrophobic unit kinetically stabilises the self-assembled nanostructures, preventing loss of binding ability in the presence of human serum – with cholesterol hydrophobic units significantly outperforming systems with a simple extended aliphatic chain. It is demonstrated that serum albumin disrupts the binding thermodynamics of the latter system. Molecular simulation shows that aliphatic lipids can more easily be removed from the self-assembled nanostructures than the cholesterol analogues. This agrees with the experimental observation that cholesterol-based systems undergo slower disassembly and subsequent degradation via ester hydrolysis than the aliphatic analogue. Furthermore, by stabilising the SAMul nanostructures, toxicity towards human cells is decreased and biocompatibility enhanced, with markedly improved survival of human hepatoblastoma cells in an MTT assay.

Introduction

Heparin is a key glycosaminoglycan polyanion associated with a wide-range of biological processes *in vivo*.[1] In particular, heparin can be used clinically to help control blood coagulation processes, of importance during major surgery where the anti-coagulant effect of heparin plays a key role.[2] Once surgery is complete, 'heparin rescue' is accomplished using protamine, a cationic highly arginylated protein, which binds to heparin as a result of electrostatic interactions, leading to heparin clearance from the bloodstream.[3] However, protamine induces adverse effects in a significant number of patients, including anaphylaxis, and has to be administered with caution in a clinical setting, particular with regard to dose levels and repeat dosing.[4] There are thus sometimes problems some hours after surgery is complete with 'heparin rebound', in which excess heparin is slowly released from plasma proteins and induces a further anti-coagulant effect.[5] There has therefore been significant interest in the development of synthetic systems which can effectively sense and/or bind heparin.[6] Heparin sensors may offer useful clinical tools to accurately detect heparin levels and avoid problems with its use, while synthetic heparin binders offer the possibility of replacing protamine in the clinic and avoiding the associated dosing problems.

Attempts to develop synthetic heparin binders date back to the 1960s, when cationic polymers were tested in this regard.[7] In the years since, other researchers have also explore a variety of elegantly designed polymers with this target in mind.[8] However, in other areas of clinical development, such as gene delivery, it has become increasingly clear that cationic polymers are not hugely desirable as a result of their toxic effects on cell membranes, and their potential long-term persistence and toxicity effects *in vivo*.[9] Small molecule heparin binders have thus also been of significant interest. Early systems were based on simple cationic dyes,[10] however, although binding heparin effectively in aqueous solution, as the level of competition is increased to include electrolytes at physiological concentrations, such systems struggle to maintain binding. The best small molecule systems incorporate significant rigidity and preorganisation such that they can most effectively use their cationic groups to bind to the heparin chain.[11] However, even still it is rare for such systems to be tested in highly biologically challenging conditions such as human serum, although some effective candidates have emerged from this work.[12]

Our interests in heparin binding have focussed on trying to combine small molecule and polymer approaches and gain the advantages of each. We have developed cationic ligands that can self-assemble to yield a multivalent ligand array (self-

[a] *Department of Chemistry, University of York, Heslington, York, YO10 5DD, UK. Email: david.smith@york.ac.uk.*
[b] *Molecular Biology and Nanotechnology Laboratory (MolBNL@UniTS), DEA, University of Trieste, Trieste, 34127, Italy. Email: SABRINA.PRICL@dia.units.it.*
Electronic Supplementary Information (ESI) available: synthesis and characterisation, assay methods and further data, details of computational simulation methods. See DOI: 10.1039/x0xx00000x

Please do not adjust margins

Please do not adjust margins

assembled multivalency = SAMul).[13] These cationic SAMul arrays show ultra-high-affinity for polyanionic biological targets.[14] In our optimal design, these ligand arrays are temporary in nature as a result of having degradable bonds within their structure.[15] On degradation, the ability of the molecule to self-assemble is lost, and the system forms small molecules with limited affinity for their binding partner. In this way, the SAMul binding effect can be temporary, ensuring that any excess heparin binder is not biopersistent, and limiting long-term or off-target toxicity effects. We have developed a range of different heparin binders and explored the fundamentals of their function, in particular focussing on aspects such as their selectivity for different polynaions (heparin and DNA),[16] the ability to tune the ligands to optimise polyanion binding and selectivity,[17] and chiral effects in the molecular recognition process.[18] In recent years, others have also begun to apply a SAMul approach to heparin binding.[19]

In addition to fundamental studies, we have also tried to develop the most effective SAMul systems against a range of important pre-clinical milestones. To date, our most effective system has been **C_{22}-G1**, which assembles into micelles at very low concentrations (4 μM) and binds heparin with ultra-high-affinity.[20] However, **C_{22}-G1** began to suffer when tested in human serum, where it underperformed in comparison with protamine. We reasoned that kinetic instability of the micelle and interaction of the alkyl chain with human serum albumin was responsible for disruption of the micellar assemblies and some loss of binding. Indeed, there has been considerable general interest in enhancing the stability of self-assembled micelles within serum with the goal of *in vivo* use,[21] and a number of strategies have emerged including the development of polymer micelles,[22] tuning of hydrophobic domains[23] and the incorporation of poly(ethylene glycol) units into self-assembled structures.[24] We wanted to enhance the stability of our micellar systems and thus targeted the synthesis of amphiphiles with a different hydrophobic unit to enhance packing, maximise stability and thus limit disruption in human serum.

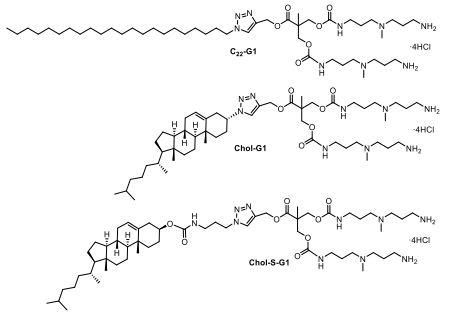

Figure 1. Structures of compounds investigated in this study.

Results and Discussion

Synthesis of SAMul ligands

We targeted the incorporation of cholesterol units, as it has previously been shown that such groups can enhance hydrophobic assembly.[25] Our first target compound was **Chol-G1**, which was synthesized using a modular approach. The Boc-protected polyamine scaffold (**G1**) with an alkyne functional group at the focal point was synthesised by a combination of different methodologies previously described by Fréchet,[26] Christensen[27] and ourselves.[28] The hydrophobic residue (**Chol**) was modified with an azide group following a two-step approach based on conversion of the alcohol to a mesylate[29] and S_N2 displacement with the azide.[30] The azide-functionalized hydrophobic unit and the alkyne-modified dendron were conjugated via a copper-catalysed 'click' reaction. Due to the steric hindrance around the azide group this reaction is slow. Furthermore, although mass spectroscopy and TLC showed the presence of just one compound, ^{1}H NMR spectra exhibited extra signals around the triazole proton chemical shift. This was also true for the Boc-deprotected product, formed by treatment with HCl in methanol. Most likely the extra NMR peaks originate because the triazole is directly attached to the cholesterol and steric hindrance generates different conformational isomers that do not readily interconvert.

This observation therefore encouraged us to modify the initial design by adding a small spacer between the cholesterol and the triazole in the hope of limiting steric hindrance and enabling greater conformational mobility. The synthesis of new target compound **Chol-S-G1** was similar to that described above for **Chol-G1**. The key difference was the incorporation of an additional spacer in the azide precursor.[31] Once again a 'click' reaction between the azide and the dendron alkyne, followed by Boc deprotection with HCl gas allowed the formation of the target compound **Chol-S-G1**. In this case the 'click' reaction was significantly faster and better yields were obtained. Finally a clear ^{1}H NMR spectra was obtained with just one signal for the triazole proton. These observations indicate that the use of a spacer does indeed alleviate the steric hindrance within **Chol-G1**. Although **Chol-G1** showed limitations, both compounds were tested for self-assembly and heparin binding. In each case, the data are compared to published data for **C_{22}-G1** in order to fully understand the impact of modification of the hydrophobic unit.

Self-assembly of SAMul ligands

Nile Red assays[32] were employed to determine the critical aggregation concentrations (CACs) of both ligands. In PBS buffer (pH 7.5), Nile Red solubilisation occurred above (8.5 ± 0.2) μM for **Chol-G1** and (6.6 ± 0.3) μM for **Chol-S-G1**. These values can be regarded as the CACs. This might suggest that **Chol-S-G1** is the slightly more effective self-assembling system. Both compounds had higher CACs than **C22-G1** analogue (4.0 μM). These data were further confirmed by Isothermal Titration Calorimetry (ITC) experiments, which yielded CAC values of 8.1 μM and 5.9 μM for the **Chol-S-G1** and the **C22-G1** systems, respectively (see ESI for details). However, all of the

This journal is © The Royal Society of Chemistry 20xx

Please do not adjust margins

obtained values are below 10 μM, which is suitable for the proposed application of heparin rescue.

The self-assembly of **Chol-G1** and **Chol-S-G1** was also assessed by transmission electron microscopy (TEM). Solutions of the compounds in water were placed on a copper grid, allowed to evaporate, and negatively stained with uranyl acetate. TEM images (Fig. 2) revealed the presence of regular spherical aggregates ca. 10 nm in diameter consistent with self-assembly into micellar systems. Computer simulations (see below) support this.

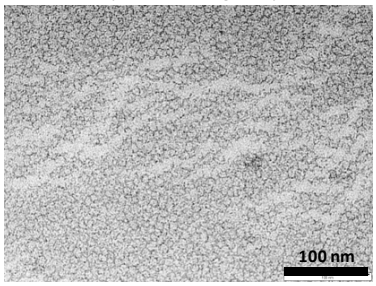

Figure 2. TEM image of **Chol-S-G1** dried from aqueous solution indicating the formation of self-assembled micellar nanostructures.

Dynamic light scattering (DLS) was in broad agreement with the observations from electron microscopy. As we have previously observed for this class of systems,[ref] the intensity distribution indicated both smaller (<10 nm) and larger (>100 nm) nanostructures. However, when correcting for the number of nanostructures in the volume distribution, the smaller nanostructures are clearly dominant. The sizes of these are (7.9 ± 0.2) nm for **Chol-G1** and (7.5 ± 0.2) nm for **Chol-S-G1**. Clearly these are similar in size, although the system incorporating the spacer unit gives slightly smaller assemblies, which might suggest more effective packing, in agreement with the lower CAC value for **Chol-S-G1**.

Heparin binding studies

In order to monitor solution-phase heparin binding, a Mallard Blue (MalB) displacement assay was employed.[33] This simple competition assay provides good preliminary insight into heparin binding. The results from the MalB assay (Table 1) are reported in terms of the effective concentration required to displace half of the MalB from its complex with heparin (EC_{50}), the charge excess of cationic binder relative to anionic heparin at this point (CE_{50}) and the effective dose of the binder (in mg per 100 international units [IU] of heparin). It should be noted that only 30-40% of heparin is constituted by the pentasaccharide sequence associated with activity. As such, the heparin concentrations refer to the total concentration of anionic disaccharide, irrespective of activity, while the dose refers only to the clinically active heparin in the sample. We benchmarked the data against the performance in the assay of **C_{22}-G1** (our best previous heparin binder) and protamine (the clinically applied heparin binder).

As indicated in Table 1, for heparin binding in aqueous buffer (Tris-HCl, 10 mM, pH 7.4) in the presence of physiological salt concentrations (NaCl, 150 mM), both **Chol-G1** and **Chol-S-G1** showed effective heparin binding, with EC_{50} values of (26.0 ± 2.0) and (21.2 ± 0.5) μM respectively. In the absence of self-assembly, such ligands are incapable of binding heparin at these low concentrations, and this can therefore clearly be classified as a SAMul binding effect, in which self-assembly is an essential prerequisite for effective multivalent binding. However, both **Chol-G1** and **Chol-S-G1** were significantly less effective heparin binders than **C_{22}-G1** (7.5 ± 1.2 μM) or the clinical agent protamine (2.3 ± 0.2 μM). It should be noted that protamine has many more charges per mole than the synthetic binders, and a fairer comparison between protamine and the SAMul systems is in terms of the CE_{50} values which reflect the amount of cationic charge required to bind anionic heparin. These CE_{50} values are 0.96, 0.72, 0.28 and 0.52 for **Chol-G1**, **Chol-S-G1**, **C_{22}-G1** and protamine respectively. Therefore, under these conditions, it is clear that **C_{22}-G1** is the most effective heparin binder in terms of using its charge, outperforming protamine, while the two new cholesterol-modified derivatives are somewhat less effective. This reflects the observation that **C_{22}-G1** is a highly effective self-assembling systems, with a low CAC.

Table 1: Heparin binding data from MalB assay in buffer TRIS-HCl 10 mM and NaCl 150 mM.

Compound	EC_{50}[a] (μM)	CE_{50}[b]	Dose[c] mg/100IU
Chol-G1	26.0 ± 2.0	0.96 ± 0.07	0.80 ± 0.06
Chol-S-G1	19.3 ± 0.5	0.79 ± 0.02	0.66 ± 0.02
C_{22}-G1	7.5 ± 1.2	0.28 ± 0.05	0.23 ± 0.04
Protamine	2.3 ± 0.2	0.52 ± 0.05	0.32 ± 0.03

a: the effective concentration required to displace half of the MalB from its complex with heparin (EC_{50}); b: the charge excess of cationic binder relative to anionic heparin at this point (CE_{50}); c: and the effective dose of the binder (in mg per 100 international units [IU] of heparin).

Further to the MalB assay, TEM studies on samples of **Chol-G1** and **Chol-S-G1** in the presence of heparin demonstrated that the SAMul assemblies remain intact and are not disrupted by heparin binding. Indeed, the cationic self-assembled micelles cluster together in a close packed manner with the polyanionic heparin (Fig. 3). Similar images have been observed by us previously for cationic SAMul micelles binding to heparin and the packing of spherical cationic micelles and

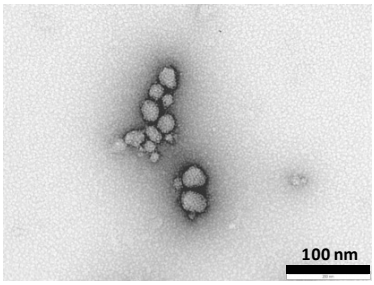

Deleted: for

Deleted: Multiscale modelling

Deleted: s

linear anionic polymers has been structurally characterised using small angle X-ray scattering methods.[34]

Figure 3. TEM image of **Chol-S-G1** in the presence of heparin dried from aqueous solution indicating the formation of self-assembled micelles that form close packed hierarchically organised nanoscale aggregates.

The assays were then performed under more biologically relevant conditions in human serum. Serum is electrolytically rich and contains all of the proteins (except those involved in blood clotting), antigens, antibodies and hormones that routinely appear in blood. The translation of any system for use *in vivo* requires effective performance in serum. The assay was performed using the same conditions as before, but the heparin was delivered in 100 % human serum instead of Tris-HCl. In this study we focussed on **Chol-S-G1** as the more effective, 'lead' binding system.

Table 2: Heparin binding data from MalB assay with heparin delivered in 100% human serum.

Compound	EC_{50}[a] (μM)	CE_{50}[b]	Dose[c] mg/100IU
Chol-S-G1	19 ± 2	0.69 ± 0.07	0.63 ± 0.07
C_{22}-G1	26 ± 2	0.96 ± 0.06	0.79 ± 0.05
Protamine	3.5 ± 0.1	0.79 ± 0.03	0.21 ± 0.01

a: the effective concentration required to displace half of the MalB from its complex with heparin (EC_{50}); b: the charge excess of cationic binder relative to anionic heparin at this point (CE_{50}); c: and the effective dose of the binder (in mg per 100 international units [IU] of heparin).

Table 2 indicates that the CE_{50} value of **Chol-S-G1** was 0.69 In contrast, the CE_{50} of **C_{22}-G1** was 0.96. Therefore in serum, **Chol-S-G1** significantly outperform **C_{22}-G1** as a heparin binders. Furthermore, protamine has a CE_{50} value of 0.79 in the human serum assay. This suggests that in these more highly competitive conditions, **Chol-S-G1** is particularly effective for heparin binding, in terms of the way it uses charge and, in contrast to **C_{22}-G1**, our previous best heparin binder, outperforms the current clinical agent, protamine.

As noted in the introduction, the self-assembly of **C_{22}-G1** may be disrupted as a result of interactions between the hydrophobic chain and serum albumins. The observed results lead us to suggest that the **Chol-S-G1** SAMul nanostructures are less disrupted by the presence of human serum and hence maintain their ability to bind heparin with high affinity. We characterise these processes further in the sections below.

Isothermal titration calorimetry (ITC) experiments

We went on to probe the heparin binding by **Chol-S-G1** and **C_{22}-G1** in more detail by isothermal titration calorimetry (ITC, see ESI). ITC was performed above the CAC value to avoid complications arising from demicellisation process energetics. ITC measurements confirmed the results obtained from MalB displacement assays, according to which the **C_{22}-G1** micelles gave the best polyanion binding (Fig. 4) in buffered conditions. Small differences (ca. 1.9 kJ/mol) were detected between the binding free energies of **C_{22}-G1** (ΔG_{obs} = -32.73 kJ/mol) and **Chol-S-G1** (ΔG_{obs} = -30.85 kJ/mol), consistent with the small differences in affinity suggested from the MalB competition assay (Table 1). For both **C_{22}-G1** and **Chol-S-G1**, binding was enthalpically favored, as a result of high-affinity electrostatic interactions between the negative charges of heparin and the SAMul cationic surface, with ΔH_{obs} values of -21.18 kJ/mol and -20.71 kJ/mol for **C_{22}-G1** and **Chol-S-G1**, respectively. As a result of the release of water and ions from the both charged surfaces upon binding, the entropic contribution ($-T\Delta S_{obs}$) also favored binding ($-T\Delta S_{obs}$ = -11.55 kJ/mol for **C22-G1** and $-T\Delta S_{obs}$ = -10.14 kJ/mol for **Chol-S-G1**, respectively).

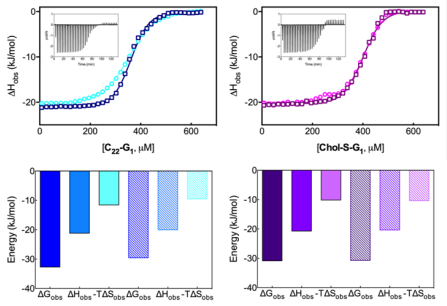

Figure 4. (Upper panel) ITC traces for the titration of **C_{22}-G1** (left) and **Chol-S-G1** (right) with heparin in absence (squares) or presence (triangles) of 500 μM of HSA. (Insets show the measured heat power vs. time elapsed during each SAMul/heparin binding in the absence of HSA as an example). (Bottom panel) Summary of thermodynamic data extracted from ITC for the binding of **C_{22}-G1** (left) and **Chol-S-G1** (right) nanosystems to heparin in absence (filled bars) or presence (patterned bars) of 500 μM of HSA.

Previously, to explain the different behavior of **C_{22}-G1** and **Chol-S-G1** in binding heparin in serum, we hypothesized that the linear alkyl derivative **C_{22}-G1** is more prone to interact with serum proteins than the **Chol-S-G1** as a result of interactions between the alkyl chain and hydrophobic protein binding sites. Since human serum is a very complex system, and its employment in calorimetric studies is extremely challenging, we reasoned that Human Serum Albumin (HSA), the most abundant protein in human plasma, could be an effective surrogate system for investigating competitive effects in heparin binding of our SAMuls. Accordingly, we repeated the same ITC experiments described above, but in the presence of 500 μM of HSA (Fig. 4).

In the presence of HSA, **Chol-S-G1** had the same binding performance exhibited in the assay in the absence of the serum protein: HSA did not significantly interfere in heparin binding and, indeed, very small differences were found in the corresponding interaction thermodynamics with the polyanion (ΔG_{obs} = -30.72 kJ/mol; ΔH_{obs} = -20.35 kJ/mol; $-T\Delta S_{obs}$ = -10.37 kJ/mol – i.e. $\Delta(\Delta G)$ = 0.13 kJ/mol, $\Delta(\Delta H)$ = 0.36 kJ/mol and $\Delta(T\Delta S)$ = 0.23 kJ/mol). On the other hand, and in agreement with the dye displacement assay, the binding of **C_{22}-G1** to heparin was affected by the presence of the HSA in solution: in this case, both the enthalpic (ΔH_{obs} = -20.03 kJ/mol) and the entropic ($-T\Delta S_{obs}$ = -9.53 kJ/mol) contributions were less favorable. Comparing these values with those measured in the absence of HSA, gives values of $\Delta(\Delta H)$ = 1.15 kJ/mol and $\Delta(T\Delta S)$ = 2.02 kJ/mol. Consequently, the overall binding free

This journal is © The Royal Society of Chemistry 20xx

energy was significantly less effective in the presence of HSA, with a ΔG_{obs} value of -29.56 kJ/mol ($\Delta(\Delta G)$ = 3.17 kJ/mol).

Degradation assays

Given the ability of **Chol-S-G1** to outperform protamine in our heparin binding assay in the presence of serum, we went on to test some of the key pharmacokinetic parameters. Firstly, we considered the degradation. Ideally, nanostructures used for intervention *in vivo* should be degradable to avoid biopersistence and hence reduce the chance of off-target or longer-term toxicity effects. For this reason, an ester bond was intentionally included in the linker between the hydrophobic unit and the hydrophilic amine ligands. The ester bond can be degraded under biological conditions of pH, or by the presence of enzymes as has been previously shown.[ref] In this way, the SAMul binding effect is temporary, and can be switched off by degradation, which then induces disassembly of the nanostructures and hence loss of the high-affinity multivalent binding.

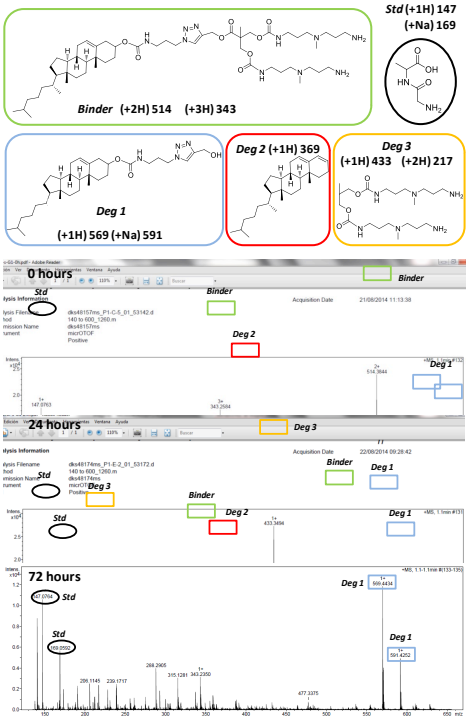

Figure 5. Structures of compounds and degradation products and masses of resulting ions. Mass spectra of **Chol-S-G1** at the start of the assay and after incubation at 25°C for 24 h and 72 h, respectively.

To confirm whether the present binders underwent the desired degradation, a mass spectrometric study was carried out (Fig. 5). The SAMul systems were dissolved in buffer at pH = 7.5 in the presence of Gly-Ala dipeptide as internal standard. Mass spectra were obtained at 0 h and after incubation at 25°C for 24 and 72 h. For **Chol-S-G1** at time = 0 h, the molecular ions for the intact compound were mostly detected (*m/z* = 514 $[M+2H]^{2+}$ and 343 $[M+3H]^{3+}$) alongside very small quantities of degradation products. After incubation for 24 h, ester hydrolysis products were dominant (alcohol, *m/z* = 569 $[X+H]^{+}$ and 591 $[X+Na]^{+}$; and decarboxylated acid dendron, *m/z* = 433 $[Y+H]^{+}$ and 217 $[Y+2H]^{2+}$), although the molecular ion for the intact dendron was still observed. This is in contrast to the previously reported degradation of $\mathbf{C_{22}}$**-G1** where no intact molecular ion was observed after 24 h. This suggests that the degradation of **Chol-S-G1** is slower than that of $\mathbf{C_{22}}$**-G1**. After incubation for 72 h, the molecular ion associated with intact **Chol-S-G1** was no longer observed. The same degradation pathway was observed for **Chol-G1** in the mass spectrometry assay (see ESI).

To demonstrate that degradation of the ligand led to disassembly of the self-assembled nanostructures we performed a Nile Red assay over time for our favoured system, **Chol-S-G1** (Fig. 6). We incubated **Chol-S-G1** in PBS buffer, in the presence of Nile Red, and monitored fluorescence intensity over time. After incubation for 24 h at room temperature, the fluorescence intensity had fallen to around 50% of its starting intensity, indicating that the self-assembled nanostructures were indeed being disrupted as a result of ligand degradation. Once again, in comparison with $\mathbf{C_{22}}$**-G1** the degradation and disassembly of **Chol-S-G1** is very significantly slower. This suggests that the cholesterol-based micelles are kinetically more stable than those based on $\mathbf{C_{22}}$**-G1**, and hence less susceptible to degradation. This would also agree with the observation above that **Chol-G1** and **Chol-S-G1** are less disrupted by serum and better able to retain their multivalent binding – kinetic stabilisation will limit the impact of competitive influences.

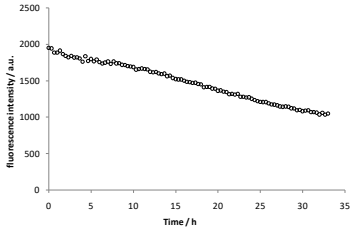

Figure 6. Degradation-induced disassembly of self-assembled nanostructures based on **Chol-S-G1** as monitored via Nile Red assay.

The degradation of **Chol-S-G1** remains potentially pharmaceutically useful. In particular, incubating the samples at 37°C led to more rapid disruption of the self-assembled nanostructures – such that excess heparin binder could be readily degraded. We have previously shown that once bound to heparin, the degradation of this family of compounds is inhibited, meaning that in clinical use, the intact complex is stable and could potentially be excreted.[ref]

Determination of micelle stability by computer simulation

To support the hypothesis that the micelles formed by **Chol-S-G1** and **C_{22}-G1** had different stabilities and to gain further insight into their kinetic stability, constant-force steered molecular dynamic simulations (CF-SMD) were performed. Precisely, we evaluated the reaction opposed by each micelle to a force applied to pull out one of their respective monomers. During each simulation, a constant force vector was applied in order to increase the distance between the center of mass of the micelle and the center of mass of a selected SAMul head. The force, constant was varied in different simulations, and the MD runs were continued until an equilibrium distance was reached for each specific applied force. In order to avoid any bias, we repeated every simulation three times for both micelle type, selecting a different SAMul unit from each micelle.

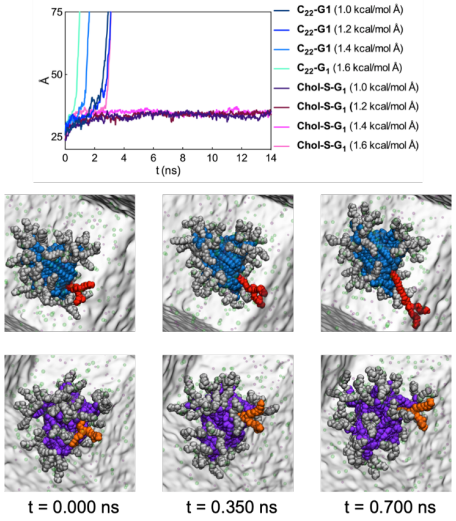

Figure 7. (Upper panel) Distance between the micelle center of mass (COM) and the COM of the SAMul head selected for pullout over simulation time during a set CF-SMD experiments. Force values applied during different CF-SMD simulation are indicated in the label (see text for more details), varying the applied force. (Lower panel) CF-SMD snapshots of **C_{22}-G1** (upper row) and **Chol-S-G1** (lower row) systems under a pulling force of 1.6 kcal/(mol Å) at three representative times. In each micelle, monomers are represented by their van der Waals radius, and colored as follows: the hydrophobic core of **C_{22}-G1** is portrayed in blue, the hydrophobic core of **Chol-S-G1** is in purple, the head portions of both SAMuls are portrayed in grey, while the pullout monomers are highlighted in red and orange for the **C_{22}-G1** and **Chol-S-G1** systems, respectively. Na^+ and Cl^- ions are represented as purple and green transparent spheres, respectively, while water is represented by a transparent grey field.

As shown in the upper panel of Figure 7, all simulations collectively confirmed the underlying hypothesis of a lower stability of the **C_{22}-G1** micelle compared with **Chol-S-G1**. Indeed, from the blue set of curves in the top panel of Figure 7, it can be readily seen that, even at the lowest pullout force applied (1.0 kcal/mol Å), a **C_{22}-G1** SAMul monomer can already be extracted from its micelle at an early stage of the simulation. In contrast, a substantially higher force must be exerted to extract a **Chol-S-G1** monomer from the corresponding self-assembled nanomicelle (1.6 kcal/mol Å, pink set of curves). No monomer pullout can be achieved when lower forces are applied. The lower panel in Figure 7 shows three CF-SMD snapshots of the monomer pullout process from the **C_{22}-G1** and **Chol-S-G1** micelles at the highest force applied and at different simulation times. As we can see from these images, the **C_{22}-G1** monomer is completely extracted from its micelles after 0.7 ns of CF-SMD (upper row) while, at the same simulation time, the **Chol-S-G1** monomer is still well inserted within the corresponding micellar structure. This clearly indicates a greater kinetic stability of the micelles using cholesterol as a hydrophobic unit.

Toxicity Assays

Finally, we determined the toxicity of these compounds in cell viability assays. Specifically we performed MTT assays,[35] a colorimetric assay based on the ability of cells to reduce a soluble yellow tetrazolium salt to bue formazan crystals. This assay was performed using human hepatoblastoma cells (Hep3B, ATCC HB-8064). Cells were exposed to the SAMul systems for 24 h in complete MEM (Minimum Essential Medium) with FBS (Fetal Bovine Serum). The MTT dye was added for the last 4 h of incubation and absorbance was detected at 570 nm.

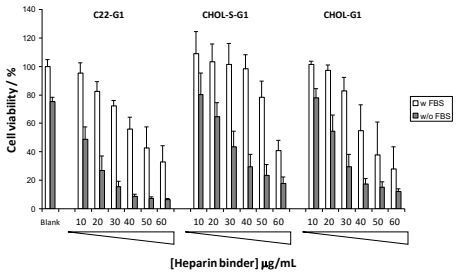

Figure 8. Percentage of cell viability in the presence of **C_{22}-G1**, **Chol-S-G1** and **Chol-G1** at a range of different concentrations. Open bars are the optimised assays in the presence of FBS throughout. Shaded bars are performed in the absence of FBS for the first 3 hours, but this had adverse effects on cell viability even in the absence of the SAMul system (see 'blank' control).

Interestingly, compound **C_{22}-G1** showed significantly higher toxicity than the cholesterol derivatives. For **C_{22}-G1**, once the dose exceeded 20 µg/mL, cell viability fell below 80%. However, for **Chol-G1** and **Chol-S-G1** the cell viability remained above 80% up to concentrations of 30 µg/mL and 50 µg/mL respectively. In the case of **Chol-S-G1** this is a practically useful level – indeed cells were completely unaffected up to concentrations of 40 µg/mL. We suggest that the flexible carbon chain in the relatively unstable **C_{22}-G1** assemblies, is subsequently able to insert into cell membranes, disrupting normal cell behaviour and causing cell death. The greater stability of **Chol-S-G1** assemblies in highly competitive conditions (see discussions above) mean this system is less able to disassemble disrupt cell membranes.

This journal is © The Royal Society of Chemistry 20xx

Please do not adjust margins

Please do not adjust margins

Conclusions

Two new potential heparin rescue agents**, Chol-G1 and Chol-S-G1**, were designed, synthesized and fully characterized. Both self-assemble in water at low concentrations. In the presence of buffer and electrolyte, these new binders were less effective than **C_{22}-G1** and protamine, having higher EC_{50} values in the MalB displacement assay. However in assays containing human serum, **Chol-S-G1** was much more effective than **C_{22}-G1** and even more effective than clinically used protamine. ITC demonstrated that the presence of human serum albumin significantly adversely affected the binding thermodynamics of **C_{22}-G1** towards heparin, but not those of **Chol-S-G1**. The SAMul nanostructures with cholesterol as the hydrophobic unit thus appear to be less disrupted in the presence of serum proteins, favouring multivalent recognition. Mass spectrometry confirmed that degradation of both **Chol-S-G1** (and **Chol-G1)** occurred through hydrolysis of the ester link between the hydrophobic and hydrophilic unit, switching off the multivalent binding properties properties of the self-assembled system. Molecular simulation methods indicated that removal of one amphiphile from the micelle was significantly easier for **C_{22}-G1** than for **Chol-S-G1**, confirming the greater stability of the latter nanostructures. Finally, both cholesterol-based compounds showed significantly lower toxicity to human cells than **C_{22}-G1**, with **Chol-S-G1** showing no evidence of toxicity up to 40 μg/mL – we suggest that the **C_{22}-G1** can insert into human cell membranes and induce cell death, whereas the more stable **Chol-S-G1** assemblies are much better tolerated. In summary, as demonstrated using this combined experimental and computational study, simple hydrophobic modification of SAMul nanosystems can significantly enhance resistance to serum, improving multivalent binding performance in these highly competitive conditions and lowering their toxicity. This approach is therefore a simple and powerful way of optimising self-assembled systems for intervention in biomedical processes, such as heparin rescue.

Conflicts of interest

There are no conflicts to declare.

Acknowledgements

M.T.-S. thanks the Ministry of Education, Culture and Sport of Spain for an FPU fellowship and mobility grant. ACR was funded by Marie Curie IEF 628757. The financial support of the Italian Association for Cancer Research (AIRC IG IG17413 to SP) is gratefully acknowledged.

Notes and references

1 D. L. Rabenstein, *Nat. Prod. Rep.* 2002, **19**, 312-331.
2 (*a*) R. Barbucci, A. Magnani, S. Lamponi and A. Albanese, *Polym. Adv. Technol.* 1996, **7**, 675-685. (*b*) S. Middeldorp, *Thromb. Res.* 2008, **122**, 753-762.
3 (*a*) R. Balhorn, *Genome Biol*. 2007, **8**, 227. (*b*) S. Schulman and N. R. Bijsterveld, *Transfus. Med. Rev.*, 2007, **21**, 37-48.
4 (*a*) M. Nybo and J. S. Madsen, *Basic Clin. Pharmacol.* 2008, **103**, 192-196. (*b*) Y.-Q. Chu, L.-J. Cai, D.-C. Jiang, D. Jia, S.-Y. Yan and Y.-Q. Wang, *Clin. Ther.* 2010, **32**, 1729-1732. (*c*) C. E. Mahan, *J. Thrombosis Thrombolysis*, 2014, **37**, 271-278. (*d*) E. Sokolowska, B. Kalaska, J. Miklosz and A. Mogielnicki, *Exp. Opin. Drug Metab. Toxicol.*, 2016, **12**, 897-909.
5 (*a*) C. Hermans and D. Claeys, *Curr. Med. Res. Opinion* 2006, **22**, 471-481. (*b*) Z. Jia, G. Tian, Y. Ren, Z. Sun, W. Lu and X. Hou, *J. Trans. Med.*, 2015, **13**, 45.
6 (*a*) S. M. Bromfield, E. Wilde and D. K. Smith, *Chem. Soc. Rev.*, 2013, 42, 9184-9195. (*b*) R. J. Weiss, J. D. Esko and Y. Tor, *Org. Biomol. Chem.*, 2017, **15**, 5656-5668.
7 (*a*) W. A. Weiss, J. S. Gilman, A. J. Catenacci and A. E. Osterberg*, J. Am. Med. Assoc.* 1958, **166**, 603-607. (*b*) C. W. Lillehei, L. P. Stems, D. M. Long and D. Lepley, *Ann. Surg.* 1960, **151**, 11-16. (*c*) G. Montalescot, W. M. Zapol, A. Carvalho, D. R. Robinson, A. Torres and E. Lowenstein, *Circulation* 1990, **82**, 1754-1764. (*d*) M. Kikura, M. K Lee and J. H. Levy, *Anesth. Analg*. 1996, **83**, 223-227.
8 (*a*) W. Sun, H. Bandmann and T. Schrader, *Chem. Eur. J.* 2007, **13**, 7701-7707. (*b*) K. Kaminski, M. Plonka, J. Ciejka, K. Szczubialka, M. Nowakowska, B. Lorkowska, T. Korbut and R, Lach, *J. Med. Chem.* 2011, **54**, 6586-6596. (*c*) B. Kalanska, E. Sokolowska, K. Kaminski, K. Szczubialka, K. Kramkowski, A. Mogielnicki, M. Nowakowska and W. Buczko, *Eur. J. Pharmacol.* 2012, **686**, 81-89. (*d*) B. Kalaska, J. Miklosz, K. Kaminski, B. Musielak, S. I. Yusa, D. Pawlak, M. Nowakowska, K. Szczubialka and A. Mogielnicki, *RSC Adv.* 2019, **9**, 3020-3029.
9 H. Lv, S. Zhang, B. Wang, S. Cui and J. Yan, *J. Controlled Rel.*, 2006, **114**, 100-109.
10 (*a*) M. D. Klein, R. A. Drongowski, R. J. Linhardt and R. S. Langer, *Anal. Biochem.* 1982, **124**, 59-64. (*b*) Q. C. Jiao, Q. Liu, C. Sun and H. He, *Talanta* 1999, **48**, 1095-1101
11 (*a*) Z. L. Zhong and E. V. Anslyn, *J. Am. Chem. Soc.* 2002, **124**, 9014-9015. (*b*) S. Choi, D, J. Clements, V. Pophristic, I. Ivanov, S. Vemparala, J. S. Bennett, M. L. Klein, J. D. Winkle and W. F. DeGrado*, Angew. Chem. Int. Ed.* 2005, **44**, 6685-6689. (*c*) T. Mecca, G. M. L. Consoli, C. Geraci, R. La Spina and F. Cunsolo, *Org. Biomol. Chem.* 2006, **4**, 3763-3768. (*d*) M. Schuksz, M. M. Fuster, J. R. Brown, B. E. Crawford, D. P. Ditto, R. Lawrence, C. A. Glass, L. Wang, Y. Tor and J. D. Esko*, Proc. Natl. Acad. Sci. USA* 2008, **105**, 13075-13080. (*e*) R. J. Weiss, P. L. S. M. Gordts, D. Le, D. Xu, J. D. Esko and Y. Tor, *Chem. Sci.*, 2015, **6**, 5984-5993. (*f*) Y. Ding, L. Shi and H. Wei, *Chem. Sci.*, 2015, **6**, 6361-6366. (*g*) S. Valimaki, N. K. Beyeh, V. Linko, R. H. A. Ras and M. A. Kostiainen, *Nanoscale*, 2018, **10**, 14022-14030.
12 (*a*) A. T. Wright, Z. L. Zhong and E. V. Anslyn, *Angew. Chem. Int. Ed.* 2005, **44**, 5679-5682. (*b*) S. L. Wang and Y. T. Chang, *Chem. Commun.* 2008, 1173-1175 (*c*) R. E. McAllister, *Circulation* 2010, **122**, A17322. (*d*) J. Kuziej, E. Litinas, D. A. Hoppensteadt, D. Liu, J. M. Walenga, J. Fareed and W. Jeske*, Clin. Appl. Thromb. Hemost.* 2010, **16**, 377-386. (*e*) S. M. Bromfield, A. Barnard, P. Posocco, M. Fermeglia, S. Pricl and D. K. Smith, *J. Am. Chem. Soc.*, 2013, **135**, 2911-2914. (*f*) J. P. Francoia, R. Pascal and L. Vial, *Chem. Commun.*, 2015, **51**, 1953-1956. (*g*) C. W. Chan and D. K. Smith, *Chem. Commun.*, 2016, **52**, 3785-3788. (*h*) U. Warttinger, C. Giese, J. Harenberg, E. Holmer and R. Krämer, *Anal. Bioanal. Chem.*, 2016, **408**, 8241-8251.
13 (*a*) A. Barnard and D. K. Smith, *Angew. Chem. Int. Ed.*, 2012, **51**, 6572-6581. (*b*) K. Petkau-Milroy and L. Brunsveld, *Org. Biomol. Chem.*, 2013, **11**, 219-232. (*c*) E. Bartolami, C. Bouillon, P. Dumy and S. Ulrich, *Chem. Commun.*, 2016, **52**,

Please do not adjust margins

Please do not adjust margins

4257-4273. (*d*) D. K. Smith, *Chem. Commun.*, 2018, **54**, 4743-4760.
14 P. Posocco, S. Pricl, S. Jones, A. Barnard and D. K. Smith, *Chem. Sci.*, 2010, **1**, 393-404.
15 A. Barnard, P. Posocco, S. Pricl, M. Calderon, R. Haag, M. E. Hwang, V. W. T. Shum, D. W. Pack and D. K. Smith, *J. Am. Chem. Soc.*, 2011, **133**, 20288–20300.
16 (*a*) S. M. Bromfield and D. K. Smith, *J. Am. Chem. Soc.*, 2015, **137**, 10056-10059. (*b*) B. Albanyan, E. Laurini, P. Posocco, S. Pricl and D. K. Smith, *Chem. Eur. J.*, 2017, **23**, 6391-6397.
17 L. Fechner, B. Albanyan, V. M. P. Vieira, E. Laurini, P. Posocco, S. Pricl and D. K. Smith, *Chem. Sci.*, 2016, **7**, 4653-4659.
18 (*a*) C. W. Chan, E. Laurini, P. Posocco, S. Pricl and D. K. Smith, *Chem. Commun.*, 2016, **52**, 10540-10543. (*b*) K. A. Thornalley, E. Laurini, S. Pricl and D. K. Smith, *Angew. Chem. Int. Ed.*, 2018, **57**, 8530-8534.
19 (*a*) K. Rajangam, H. A. Behanna, M. J. Hui, X. Han, J. F. Hulvat, J. W. Lomasney and S. I. Stupp, *Nano Lett.*, 2006, **6**, 2086-2090. (*b*) G. L. Montalvo, Y. Zhang, T. M. Young, M. J. Costanzo, K. B. Freeman, J. Wang, D. J. Clements, E. Magavern, R. W. Kavash, R. W. Scott, D. H. Liu and W. F. DeGrado, *ACS Chem. Biol.*, 2014, **9**, 967-975. (*c*) T. Noguchi, B. Roy, D. Yoshihara, J. Sakamoto, T. Yamamoto and S. Shinkai, *Angew. Chem. Int. Ed.,* 2016, **55**, 5708-5712. (*d*) H. Y. Cheong, M. Groner, K. Hong, B. Lynch, W. R. Hollingsworth, Z. Polonskaya, J.-K. Rhee, M. M. Baksh, M. G. Finn, A. J. Gale and A. K. Udit, *Biomacromolecules*, 2017, **18**, 4113-4120.
20 S. M. Bromfield, P. Posocco, C. W. Chan, M. Calderon, S. E. Guimond, J. E. Turnbull, S. Pricl and D. K. Smith, *Chem. Sci.*, 2014, **5**, 1484-1492
21 (*a*) S. Kim, Y. Shi, J. Y. Kim, K. Park and J.-X. Cheng, *Exp. Opin. Drug Deliv.*, 2010, **7**, 49-62. (*b*) Y. Lu, E. Zhang, J. Yang, Z. Cao, *Nano Res.*, 2018, **11**, 4985-4998.
22 (*a*) J. Lu, S. C. Owen, M. Shoichet, *Macromolecules*, 2011, **44**, 6002-6008. (*b*) S. C. Owen, D. P. Y. Chan and M. S. Shoichet, *Nano Today*, 2012, **7**, 53-65. (*c*) W. Zhou, C. Li, Z. Wang, W. Zhang and J. Liu, *J. Nanoparticle Res.*, 2016, **18**, 275.
23 (*a*) A. B. E. Attia, Z. Y. Ong, J. L. Hedrick, P. P. Lee, P. L. R. Ee, P. T. Hammond and Y.-Y. Yang, *Curr. Opin. Coll. Interface Sci.*, 2011, **16**, 182-194. (*b*) Z. Ahmad, A. Shah, M. Siddiq and H.-B. Kraatz, *RSC Adv.*, 2014, **4**, 17028-17038.
24 (*a*) J. Logie, S. C. Owen, C. K. McLaughlin and M. S. Shoichet, *Chem. Mater.*, 2014, **26**, 2847-2855. (*b*) H.-j. Hsu, Y. Han, M. Cheong, P. Kral and S. Hong, *Nanomedicine – Nanotechnol. Biol. Med.*, 2018, **14**, 1879-1889.
25 (*a*) C. Kirby, J. Clarke, G. Gregoriadis, *Biochem. J.*, 1980, **186**, 591-598. H. Yin, H. C. Kang, K. M. Huh and Y. H. Bae, *Coll. Surf. B*, 2014, **116**, 128-137.
26 E. R. Gillies and J. M. J. Frechet, *J. Am. Chem. Soc.*, 2002, **124**, 14137-14146
27 M. Pittelkow, R. Lewinsky and J. B. Christensen, *Synthesis* 2002, 2195-2202
28 D. J. Welsh, S. P. Jones and D. K. Smith, *Angew. Chem. Int. Ed.*, 2009, **48**, 4047-4051.
29 D. Alberti, A. Toppino, S. Geninatti Crich, C. Meraldi, C. Prandi, N. Protti, S. Bortolussi, S. Altieri, S. Aime and A. Deagostino, *Org. Biomol. Chem.*, 2014, **12**, 2457-2467.
30 D. Izhaky and L. Addadi, *Chem. Eur. J.*, 2000, **6**, 869-874
31 S. P. Jones, N. P. Gabrielson, D. W. Pack and D. K. Smith, *Chem. Commun.*, 2008, 4700-4702.
32 M. C. A. Stuart, J. C. van de Pas and J. B. F. N. Engberts, *J. Phys. Org. Chem.* 2005, **18**, 929-934.
33 S. M. Bromfield, P. Posocco, M. Fermeglia, S. Pricl, J. Rodríguez-López and D. K. Smith, *Chem. Commun.*, 2013, **49**, 4830-4832
34 V. M. P. Vieira, V. Liljeström, P. Posocco, E. Laurini, S. Pricl, M. A. Kostiainen and D. K. Smith, *J. Mater. Chem. B*, 2017, **5**, 341-347.
35 T. Mosmann, *J. Immunol. Methods*, 1983, **65**, 55-63

 This journal is © The Royal Society of Chemistry 20xx

Please do not adjust margins

Please do not adjust margins

Self-assembled multivalent (SAMul) ligand systems with enhanced stability in the presence of human serum

Graphical abstract

Modification of the hydrophobic unit of self-assembled multivalent systems limits their disruption, making them more resistant to human serum.

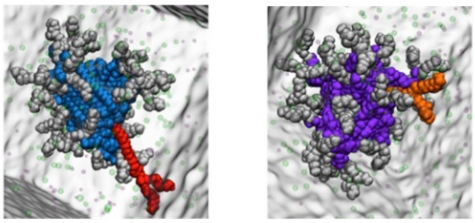

This journal is © The Royal Society of Chemistry 20xx

Please do not adjust margins